**Online Supplemental Materials**

# Novel junctophilin-2 mutation A405S is associated with basal septal hypertrophy and diastolic dysfunction

Ann P. Quick, Andrew P. Landstrom, Qiongling Wang, David L. Beavers, Julia O. Reynolds, Giselle Barreto-Torres, Viet Tran, Jordan Showell, Leonne E. Philippen, Shaine A. Morris, Darlene Skapura, J. Martijn Bos, Steen E. Pedersen, Robia G. Pautler, Michael J. Ackerman, Xander H.T. Wehrens

## Supplemental Methods

**Comprehensive genetic analysis of JPH2 in a large cohort of subjects with HCM.** Following receipt of informed consent and enrollment of the subjects into this IRB-approved study, DNA was subjected to genotyping of all five translated exons, with flanking intronic regions of *JPH2*. Each PCR amplicon was evaluated for mutations using denaturing high performance liquid chromatography (DHPLC, Transgenomic, Omaha, NE), and samples with an abnormal elution profile were directly sequenced (ABI Prism 377; Applied Biosystem, Foster City, CA) to characterize the difference between the wild type and variant alleles. Within this cohort, comprehensive direct sequencing analysis of the nine canonical genes associated with sarcomeric HCM including *MYH7*-encoded beta myosin heavy chain, *MYBPC3*-cardiac myosin binding protein C, *MYL2*-encoded regulatory myosin light chain, *MYL3*-encoded essential myosin light chain, *TNNT2*-encoded cardiac troponin T, *TNNI3*-encoded cardiac troponin I, *TNNC1*-encoded cardiac troponin C, *TPM1*-encoded alpha-tropomyosin, and *ACTC*-encoded alpha-cardiac actin (Transgenomic Inc, New Haven, CT). Genetic causes of cardiac disease which can mimic HCM – so called phenocopy - including *PRKAG2*-encoded gamma-regulatory subunit of AMP-activated protein kinase, *GLA*-encoded alpha-galactosidase A, and *LAMP2*-encoded lysosome-associated membrane protein were also comprehensively genotyped.

To confirm absence of putatively pathogenic mutations in ostensibly healthy individuals, presence of the mutation was analyzed in 1,000 reference alleles (*N* = 500 subjects). Control genomic DNA was obtained from the European Collection of Cell Cultures (HPA Culture Collections, UK), the Human Genetic Cell Repository sponsored by the National Institute of General Medical Sciences, and the Coriell Institute for Medical Research (Camden, NJ). Further, absence of the mutation in all publically-held databases including the 1,000 Genome Project (*N* = 1,094 subjects) comprised of 381 whites, 246 blacks, 286 Asians, and 181 Hispanics (1); the National Heart, Lung, and Blood Institute GO Exome Sequencing Project (n = 5,379 subjects) comprise of 3510 whites and 1869 blacks;(2) the 12000 Exome Chip (n = 12,000 subjects) (2); and the ExAC database (n = 60,706)(3). In total, putatively pathogenic variants were absent in approximately 79,679 subjects and 159,358 reference alleles.

**Pseudo-knock-in (PKI) mouse line generation.** Cardiomyocyte-specific (αMHC) JPH2-A399S overexpression transgenic (Tg) mice had a 3.9-fold increase in JPH2 expression compared to nontransgenic (NTg) controls (P=0.002). Tg mice were intercrossed with tamoxifen-inducible αMHC-driven mER-cre-mER (MCM), and conditional JPH2 knockdown mice that express a small hairpin RNA (shRNA) against JPH2 as described previously(4). The resulting triple transgenic mice (A399S PKI mice) exhibit cardiac JPH2 levels similar to NTg control mice (P>0.999, see **Sup. Fig. 2**). Similar to JPH2-A399S Tg mice, JPH2-WT Tg mice exhibited a 3.3-fold increase in JPH2 levels compared to NTg controls (P=0.002). WT PKI mice were generated by crossing αMHC-driven WT JPH2 overexpressing Tg transgenic mice with MCM and JPH2 inducible knockdown mice. WT PKI mice had JPH2 levels similar to NTg controls (P>0.999, **Sup. Fig. 2**). MCM (NTg) and WT PKI mice were used as controls. Tamoxifen was administered as previously described(4). Tamoxifen was administered intraperitoneally for 3 days to adult mice >8 weeks of age. Mice were studied 8 weeks after tamoxifen administration.

**Echocardiography.** Mice were anesthetized with 2% Isoflurane and underwent transthoracic

echocardiography using the VisualSonics Vevo 2100 Imaging System with a high frequency (30 Mhz) probe. B-mode short axis images and M-mode scans were collected as described(5). Briefly, mice chests were depilated using Nair crème, and mice were placed supine on a heated ECG board. Temperature was maintained between 36.5 ºC and 37.5 ºC, and heart rate was maintained above 400 beat per minute in order to circumvent the confounding effects of hypothermia and bradycardia.

Due to the nature of septal hypertrophy in the murine model, a novel echocardiographic imaging plane was developed to allow for comprehensive imaging of the left ventricular outflow tract in long axis. The mouse was positioned with a 45 degree leftward tilt on the imaging board with a roll of gauze supporting the midsection. The probe was tilted approximately 15 degrees forward and 45 degrees out to the left of the boom. The imaging plane was adjusted so that the outflow tract and papillary muscles in addition to the full width of the septum were in view. Imaging and analysis were performed using Vevo systems (VisualSonics, Toronto, Canada).

**Magnetic resonance imaging.** Cardiac MRI was performed as described(6). Mice were anesthetized and loaded head first and prone into a dedicated mouse coil in a Bruker Biospin 9.4T magnet. ParaVision 5.1 software was used in tandem with self-gating IntraGate software (Bruker, Ettlingen, Germany) for cardiac imaging. After a localizing scan, 1-mm long-axis bright blood fast low angle shot (FLASH) cine slices were imaged followed by perpendicular 1-mm short-axis slices using a field of view of 3.5mm x 3.5mm. Data was analyzed using Amira software (FEI Visualization Sciences Group, Bordeaux) and cvi42 (Diagnosoft, Inc, Morrisville, NC).

**Histology.** Mouse hearts were excised and perfused in 30mM KCl followed by 10% buffered formalin. 5-µm transverse and longitudinal paraffin sections were sliced and dried on slides at 37 ºC overnight. Myocytes were stained with hematoxylin and eosin or Masson's trichrome (Richard Allen Scientific). Images were photographed at 1x and 40x on a light microscope and gross morphology and myofibril

disarray were assessed qualitatively. For Masson's trichrome sections, fibrosis in the interventricular septum was analyzed using Image J. Sections were stained with FITC-labeled wheat germ agglutinin to determine intraventricular septum and free wall cardiomyocyte crossectional area, which was analyzed using Image J(7).

**Myocyte isolation.** Mouse hearts were removed following isoflurane anesthesia and rinsed in KB solution (90 mmol/L KCl, 30 mmol/L K2HPO$_4$, 5 mmol/L MgSO$_4$, 5 mmol/L pyruvic acid, 5 mmol/L β-hydroxybutyric acid, 5 mmol/L creatine, 20 mmol/L taurine, 10 mmol/L glucose, 0.5 mmol/L EGTA, 5 mmol/L HEPES, pH 7.2). The heart was cannulated through the aorta and perfused using a Langendorff setup with 0 $Ca^{2+}$ Tyrode (3 ~ 5 minutes, 37 °C), then 0 $Ca^{2+}$ Tyrode containing Liberase TH Research Grade (Roche Applied Science) for 10-15 minutes at 37 °C. After digestion, the heart was perfused with 3 ml KB solution to wash out collagenase. Then the hearts were minced in KB solution, gently agitated, then filtered through a 210μm polyethylene mesh. After settling, ventricular myocytes were washed once with KB solution, and stored in KB solution at room temperature before use.

**Confocal $Ca^{2+}$ imaging.** Ventricular myocytes were incubated with 2 $\mu$M Fluo-4-acetoxymethyl ester (Fluo-4 AM, Invitrogen) in KB solution for 30 minutes at room temperature(8). The cells were washed with dye-free normal Tyrode solution (1.8 mmol/L $Ca^{2+}$) for 20 minutes for de-esterification. Cells were transferred to a chamber equipped with a pair of parallel platinum electrodes on a laser scanning confocal microscope (LSM 510, Carl Zeiss) with a 40X oil immersion objective. Fluo-4 was excited at 488 nm with emission collected through a 515 nm long pass filter. Fluorescence images were recorded in line-scan mode with 1024 pixels per line at 500 Hz. After being paced at 1 Hz for at least 2 minutes, only myocytes showing clear striation and normal contractility were selected for further experiments. Steady state SR $Ca^{2+}$ load was estimated by rapid application of 10 mmol/L caffeine after pacing. Once steady state $Ca^{2+}$ transient was observed, pacing was stopped and $Ca^{2+}$ sparks were counted.

**T-Tubule analysis**. T-Tubules of ventricular myocytes were visualized by Di-8-ANEPPS staining (5 $\mu$mol/L for 10 min) in normal Tyrode solution with 1.8 mmol/L $Ca^{2+}$(8). Quantitative analysis of spatial integrity of T-tubules was modified from previous studies(8,9), and was performed with ImageJ software (http://rsb.info.nih.gov/ij/). Briefly, region of interest was selected within a cell and outside of nucleus. Power spectrum was computed using Fast Fourier Transform (FFT).

**Western Blotting.** Mouse tissue lysates were subjected to sodium dodecyl sulfate (SDS) polyacrylamide gel electrophoresis and transferred onto polyvinyl difluoride (PVDF) membranes. The membranes were probed with antibodies against the following targets: JPH2 (1:1,000; custom-made)(10) and GAPDH (Millipore, Temecula, CA). Membranes were incubated with secondary anti-mouse or anti-rabbit antibodies conjugated to Alexa-Fluor 680 (Invitrogen Molecular Probes, Carlsbad, CA) and IR800Dye (Rockland Immunochemicals, Gilbertsville, PA), respectively. Bands were visualized on an Odyssey infrared scanner (Li-Cor, Lincoln, NE) and quantified using ImageJ Data Acquisition Software (National Institute of Health, Bethesda, MD).

**Langendorff perfusion and hemodynamics.** Cardiac contractility and relaxation were determined as described.(11) Hearts were isolated from mice, connected to a Langendorff apparatus via the aorta, and subsequently perfused with Krebs-Henseleit buffer containing (in mmol/L) 118 NaCl, 4.8 KCl, 1.2 $KH_2PO4$, 1.25 $CaCl_2$, 1.2 $MgSO_4$, 25 $NaHCO_3$, pH 7.35 ± 0.05, and 11 glucose, bubbled with gas (95% $O_2$/5% $CO_2$). A deflated water-filled balloon made of plastic film was inserted into the left ventricle for monitoring of left ventricular pressure and rate of contraction (dP/dt). Initial left ventricular end diastolic pressure (LVEDP) was set to 5 mmHg before the beginning of the experiment. Continuous ECG measurements were recorded using a special ECG sensor placed on the surface of the Langendorff-perfused hearts. All determinations of ventricular performance were obtained using LabChart 7.0 Pro Software (ADInstruments, Colorado Springs, Colorado, USA).

**References**


1. Genomes Project C, Abecasis GR, Auton A et al. An integrated map of genetic variation from 1,092 human genomes. Nature 2012;491:56-65.
2. Fu W, O'Connor TD, Jun G et al. Analysis of 6,515 exomes reveals the recent origin of most human protein-coding variants. Nature 2013;493:216-20.
3. Lek M, Karczewski K, Minikel E et al. Analysis of protein-coding genetic variation in 60,706 humans. bioRxiv 2015.
4. Beavers DL, Wang W, Ather S et al. Mutation E169K in junctophilin-2 causes atrial fibrillation due to impaired RyR2 stabilization. J Am Coll Cardiol 2013;62:2010-9.
5. Respress JL, Wehrens XH. Transthoracic echocardiography in mice. J Vis Exp 2010:1738.
6. Heijman E, de Graaf W, Niessen P et al. Comparison between prospective and retrospective triggering for mouse cardiac MRI. NMR Biomed 2007;20:439-47.
7. Schneider CA, Rasband WS, Eliceiri KW. NIH Image to ImageJ: 25 years of image analysis. Nat Methods 2012;9:671-5.
8. Reynolds JO, Chiang DY, Wang W et al. Junctophilin-2 is necessary for T-tubule maturation during mouse heart development. Cardiovasc Res 2013;100:44-53.
9. van Oort RJ, Garbino A, Wang W et al. Disrupted junctional membrane complexes and hyperactive ryanodine receptors after acute junctophilin knockdown in mice. Circulation 2011;123:979-88.
10. van Oort RJ, Respress JL, Li N et al. Accelerated development of pressure overload-induced cardiac hypertrophy and dysfunction in an RyR2-R176Q knockin mouse model. Hypertension 2010;55:932-8.
11. Barreto-Torres G, Parodi-Rullan R, Javadov S. The role of PPARalpha in metformin-induced attenuation of mitochondrial dysfunction in acute cardiac ischemia/reperfusion in rats. Int J Mol Sci 2012;13:7694-709.

**Supplemental Table 1. Summary of M-mode echocardiographic parameters of WT and A399S mice at 8-weeks post tamoxifen.**

| | WT (n=10) | A399S (n=10) | P-Value |
|---|---|---|---|
| HR (bpm) | 452.0 IQR 411.8-533.0 | 443.4 IQR 428.5-475.0 | 0.853 |
| EF (%) | 55 IQR 54-56 | 52 IQR 48-56 | 0.165 |
| FS (%) | 29 IQR 27-31 | 27 IQR 21-24 | 0.105 |
| LVOD;d (mm) | 5.83 IQR 5.79-5.94 | 5.93 IQR 5.70-6.14 | 0.393 |
| LVID;d (mm) | 4.11 IQR 3.84-4.36 | 4.02 IQR 3.92-4.14 | 0.684 |
| IVS;d (mm) | 0.84 IQR 0.78-0.91 | 0.93 IQR 0.86-1.07 | 0.075 |
| IVS;s (mm) | 1.07 IQR 0.98-1.03 | 1.12 IQR 1.03-1.16 | 0.529 |
| LVPW;d (mm) | 0.88 IQR 0.73-0.82 | 0.90 IQR 0.82-0.97 | 0.529 |
| LVPW;s (mm) | 1.10 IQR 1.03-1.20 | 1.08 IQR 1.04-1.13 | 0.493 |

M-mode echocardiographic measurements reported as median and interquartile range (IQR) for EF, ejection fraction; FS, fractional shortening; HR, heart rate; IVS;d, interventricular septal diastolic diameter; IVS;s, interventricular septal systolic diameter; LVID;d, left ventricular internal diastolic diameter; LVOD;d, left ventricular outer diastolic diameter; LVPW;d, diastolic left ventricular posterior wall diameter; LVPW;s, systolic left ventricular posterior wall diameter. Data are expressed as mean±SEM. *P<0.05 A399S vs WT.

**Supplementary Table 2. MRI Parameters of WT and A399S Mice at 8 Weeks Post Tamoxifen.**

| | WT | n | A399S | n | p-value |
|---|---|---|---|---|---|
| **IVSD;$d_{max}$ (mm)** | 0.81 IQR 0.71-0.95 | 9 | 1.09 IQR 1.02-1.21 | 11 | <0.001 |
| **LV Mass (g)** | 0.073 IQR 0.069-0.076 | 9 | 0.091 IQR 0.085-0.099 | 10 | 0.013 |
| **EF (%)** | 60 IQR 54-67 | 9 | 56 IQR 53-61 | 11 | 0.656 |
| **BW (g)** | 30.8 IQR 30.6-32.6 | 3 | 29.7 IQR 27.7-32.7 | 10 | 0.376 |

Measurements reported as median and interquartile range (IQR) for the MRI cohort for BW: body weight, and measurements from MRI analysis including EF: ejection fraction; IVSD;$d_{max}$: maximum end diastolic interventricular septum diameter; LV Mass: end diastolic left ventricular mass. N=number animals.

**Supplemental Figure 1. Electrocardiogram of proband with A405S mutation in junctophilin-2.** Twelve-lead electrocardiogram (ECG) recorded from the proband at the age of 16 years, showing sinus rhythm with left anterior fascicular block with ST segment and T wave abnormalities, and a correct QT interval (QTc) of ~510 ms.

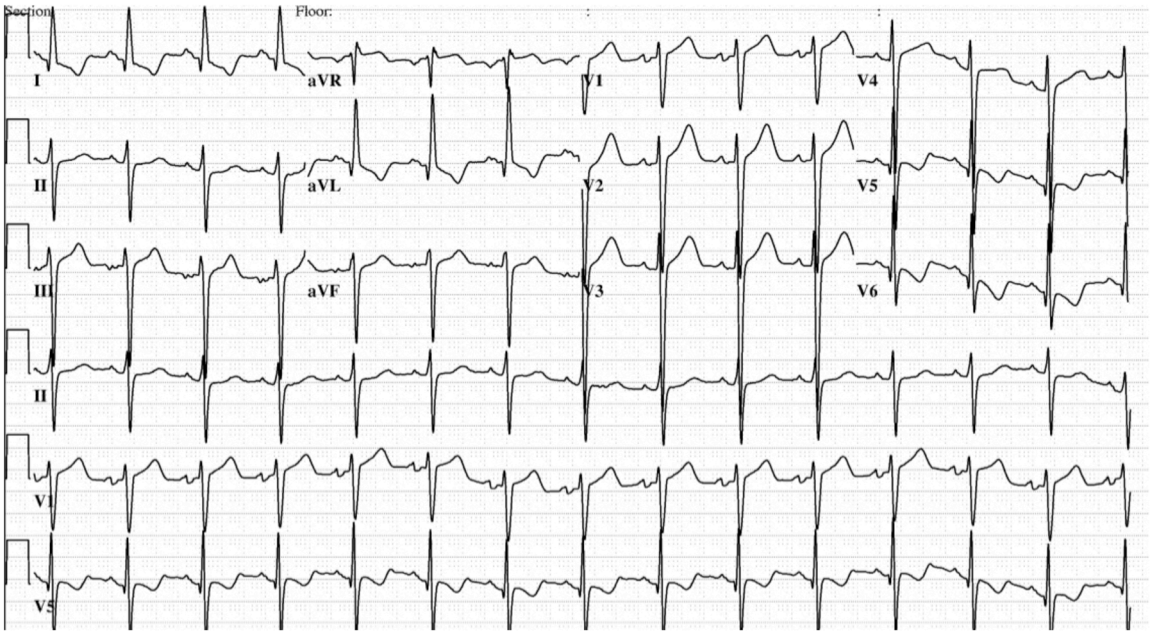

**Supplemental Figure 2. Development of pseudo-knockin (PKI) mouse lines. A.** Cartoon of the mouse alleles that were intercrossed to generate the WT-JPH2 and A399S-JPH2 PKI mouse lines**. B.** Western blot showing levels of JPH2 in the hearts of non-transgenic (NTg), transgenic (Tg), and PKI mice. **C.** Quantification of protein levels. NTg: non-transgenic; Tg: transgenic; PKI: pseudo-knock-in. N = number of mice. **P<0.01 compared to nTg.

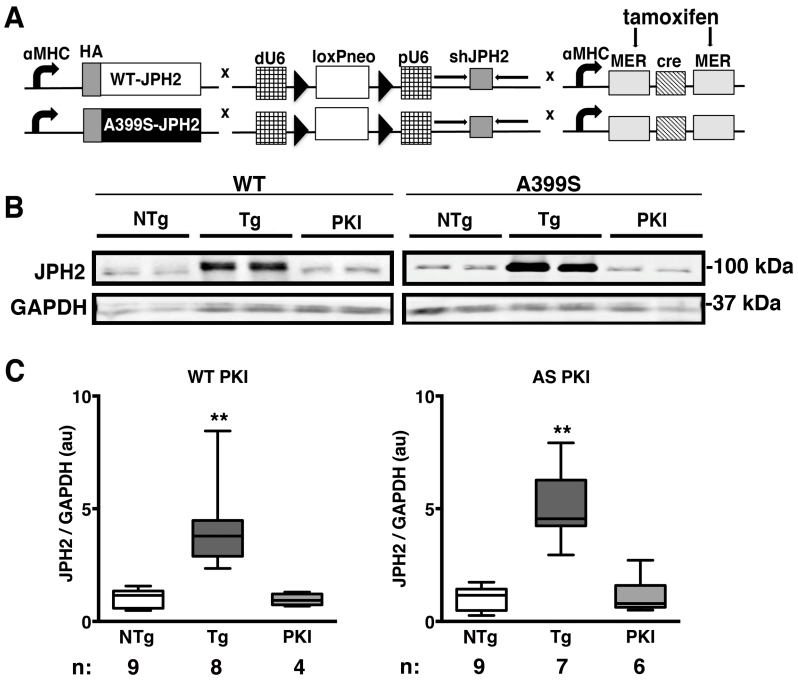

**Supplemental Figure 3. A399S PKI mice develop diastolic dysfunction.** Intra-ventricular pressure measurements were performed in the left ventricle of Langendorff perfused hearts isolated from WT-PKI and A399S-PKI mice 8 weeks after tamoxifen treatment. **A**. Plot of minimum first derivative of left ventricular pressure (dP/dt). **B**. Left ventricular end diastolic pressure (LVEDP). N = number timepoints and number in parentheses = number animals.